




ORIGINAL ARTICLE

Mitochondrial amidoxime-reducing component 1 p.Ala165Thr increases protein degradation mediated by the proteasome

Tanmoy Dutta¹  | Kavitha Sasidharan¹ | Ester Ciociola¹ | Grazia Pennisi^{1,2} |
 Francesca R. Noto^{1,3} | Lohitesh Kovooru¹ | Tobias Kroon⁴ | Anna Lindblom⁴ |
 Yue Du⁵ | Mohammad Pirmoradian⁶ | Simonetta Wallin⁴ | Rosellina M. Mancina¹  |
 Daniel Lindén^{4,7} | Stefano Romeo^{1,3,8} 

¹Department of Molecular and Clinical Medicine, Institute of Medicine, The Sahlgrenska Academy, Wallenberg Laboratory, University of Gothenburg, Gothenburg, Sweden

²Section of Gastroenterology and Hepatology, Dipartimento Di Promozione Della Salute, Materno Infantile, Medicina Interna e Specialistica Di Eccellenza (PROMISE), University of Palermo, Palermo, Italy

³Department of Medical and Surgical Sciences, University Magna Graecia, Catanzaro, Italy

⁴Bioscience Metabolism, Research and Early Development Cardiovascular, Renal and Metabolism (CVRM), BioPharmaceuticals R&D, AstraZeneca, Gothenburg, Sweden

⁵Discovery Sciences, BioPharmaceuticals R&D, AstraZeneca, Cambridge, United Kingdom

⁶Translational Science and Experimental Medicine, Research and Early Development Cardiovascular, Renal and Metabolism (CVRM), BioPharmaceuticals R&D, AstraZeneca, Gothenburg, Sweden

⁷Division of Endocrinology, Department of Neuroscience and Physiology, Sahlgrenska Academy, University of Gothenburg, Gothenburg, Sweden

⁸Department of Cardiology, Sahlgrenska University Hospital, Gothenburg, Sweden

Correspondence

Stefano Romeo, Department of Molecular and Clinical Medicine, The Sahlgrenska Academy, University of Gothenburg, Wallenberg Laboratory, Bruna Stråket 16, SE-413 45 Göteborg, Sweden.
 Email: stefano.romeo@wlab.gu.se

Funding information

AstraZeneca Agreement for Research, and AstraZeneca Cosolve; the Swedish Research Council, Grant/Award Number: 2023-02079; Swedish Government and the County Councils, Grant/Award Number: ALFGBG-965360; the Swedish Heart Lung Foundation, Grant/Award Number: 20220334; the Wallenberg

Abstract

Objective: Metabolic dysfunction-associated steatotic liver disease (MASLD) is a global health concern with no effective and specific drug treatment available. The rs2642438 minor allele in *mitochondrial amidoxime-reducing component 1* (MARC1) results in an aminoacidic substitution (p.Ala165Thr) and associates with protection against MASLD. However, the mechanisms behind this protective effect are unknown. In this study, we examined the consequences of this aminoacidic substitution on protein stability and subcellular localization.

Methods: We overexpressed the human MARC1 A165 (wild-type) or 165T (mutant) in vivo in mice and in vitro in human hepatoma cells (HepG2 and HuH-7), generated

Abbreviations: 165T, threonine at position 165 (mutant); A165, alanine at position 165 (wild-type); AAV, adeno-associated virus; ACTB, beta-actin; ALT, alanine aminotransferase; AST, aspartate aminotransferase; ATF6, activating transcription factor 6; CHX, cycloheximide; CQ, chloroquine; DBEQ, dibenzylquinazoline-2,4-diamine; ECL, enhanced chemiluminescence; ERAD, endoplasmic reticulum-associated degradation; FAFL4, fatty acid-CoA ligase 4; GCKR, glucokinase regulator; GWAS, genome-wide association study; hMARC1, human mitochondrial amidoxime-reducing component 1; IP, immunoprecipitation; IRE1, endoribonuclease inositol-requiring enzyme 1; ITR, inverted terminal repeats; MAM, mitochondria-associated membrane; MARC1, mitochondrial amidoxime-reducing component 1; MASLD, metabolic dysfunction-associated steatotic liver disease; MBOAT7, membrane bound o-acyltransferase domain containing 7; mMARC1, mouse mitochondrial amidoxime-reducing component 1; ORO, oil-red-o staining; PERK, protein kinase R-like endoplasmic reticulum (ER) kinase; PNPLA3, patatin-like phospholipase domain-containing protein 3; RTA, relative total abundance; RU, relative unit; SD, standard deviation; SDS, sodium dodecyl sulphate; SDS-PAGE, sodium dodecyl sulphate-polyacrylamide gel electrophoresis; SEM, standard error of mean; TM6SF2, transmembrane 6 superfamily member 2; UBC, ubiquitin C; UBE2E1, ubiquitin conjugating enzyme E2-E1; UBE3EC, ubiquitin protein ligase E3C; UPR, unfolded protein response; UPS, ubiquitin-mediated proteasomal (degradation) system; VCP, Valosin-Containing Protein.

This is an open access article under the terms of the [Creative Commons Attribution](https://creativecommons.org/licenses/by/4.0/) License, which permits use, distribution and reproduction in any medium, provided the original work is properly cited.

© 2024 The Authors. *Liver International* published by John Wiley & Sons Ltd.

Academy Fellows from the Knut and Alice Wallenberg Foundation, Grant/Award Number: KAW 2017.0203; the Novonordisk Distinguished Investigator Grant-Endocrinology and Metabolism, Grant/Award Number: NNF23OC0082114; the Novonordisk Project grants in Endocrinology and Metabolism, Grant/Award Number: NNF20OC0063883; the Swedish Cancerfonden, Grant/Award Number: 222270Pj

Handling Editor: Luca Valenti

several mutants at position 165 by in situ mutagenesis and then examined protein levels. We also generated HepG2 cells stably overexpressing MARC1 A165 or 165T to test the effect of this substitution on MARC1 subcellular localization.

Results: MARC1 165T overexpression resulted in lower protein levels than A165 both in vivo and in vitro. Similarly, any mutant at position 165 showed lower protein levels compared to the wild-type protein. We showed that the 165T mutant protein is poly-ubiquitinated and its degradation is accelerated through lysine-48 ubiquitin-mediated proteasomal degradation. We also showed that the 165T substitution does not affect the MARC1 subcellular localization.

Conclusions: This study shows that alanine at position 165 in MARC1 is crucial for protein stability, and the threonine substitution at this position leads to a hypomorphic protein variant due to lower protein levels. Our result supports the notion that lowering hepatic MARC1 protein level may be a successful therapeutic strategy for treating MASLD.

KEYWORDS

fatty liver, MASH, MASLD, molybdenum cofactor (MOCO) sulfuryase C-terminal domain-containing protein 1 (MOSC1), MOSC domain-containing protein 1, MTARC1, NAFLD, NASH

1 | INTRODUCTION

Metabolic dysfunction-associated steatotic liver disease (MASLD), previously termed nonalcoholic fatty liver disease (NAFLD),¹ is a heavy global burden with an estimated quarter of the global population affected.²⁻⁴ MASLD encompasses a wide spectrum of complications and can progress to steatohepatitis, end stage liver disease and hepatocellular carcinoma.^{5,6} Although there are strategies to effectively reduce liver fat and comorbidities, approved treatments are still lacking.^{7,8} In this context, the identification of novel therapies is of utmost importance.

MASLD has a strong genetic component with a common genetic variant in *PNPLA3* having the largest robust effect size.⁹⁻¹¹ There are many other common variants contributing to the risk of MASLD in *TM6SF2*, *GCKR* and *MBOAT7*.¹²⁻¹⁴ A genome-wide association study (GWAS) identified a variant (rs2642438) in the mitochondrial amidoxime-reducing component 1 (*MARC1*, also known as *MTARC1*) gene. The rs2642438 minor allele associates with lower liver triglycerides content and transaminases level and confers protection against cirrhosis and hepatocellular carcinoma.^{15,16} Mass spectrometric analysis revealed that carriers of the minor allele have higher concentrations of hepatic polyunsaturated phosphatidylcholines compared to non-carriers.¹⁷ Interestingly, the protective effect conferred by the mitochondrial amidoxime-reducing component 1 (*MARC1*) minor allele is also present against alcoholic liver disease.¹⁸ *MARC1* encodes for a molybdenum containing enzyme localized to the outer mitochondrial membrane, that has reductive activity and converts nitrate to nitric oxide.^{19,20} However, the physiological role of *MARC1* in hepatic triglycerides homeostasis remains to be elucidated.

The *MARC1* rs2642438 variant is a single nucleotide change resulting in an alanine (A) to threonine (T) substitution at position 165 of

Key points

We investigated a genetic variation (rs2642438) that protects against liver diseases. This variation causes a single amino acid change in mitochondrial amidoxime-reducing component 1 (*MARC1*) and results in its lower protein levels, making it less effective. This may be a successful therapeutic strategy to maintain liver health by lowering liver *MARC1* level.

the protein. However, the consequences of this aminoacidic change on protein function, stability and subcellular localization are not known.

Therefore, in the present study we attempt to elucidate whether the *MARC1* A165T aminoacidic change results in either a loss or gain of function. Our data reveal that overexpression of the *MARC1* 165T mutant protein results in lower protein levels compared to the overexpression of the A165 wild-type protein. The lower 165T protein level is the result of reduced protein stability due to accelerated proteasomal degradation, while there is no difference in subcellular localization. In conclusion, our data show that the A165T results in a loss of *MARC1* function.

2 | MATERIALS AND METHODS

2.1 | Animals

All experimental procedures were approved by the Gothenburg ethics review committee on animal experiments. Female C57Bl/6N mice were purchased at 7–8 weeks of age from Charles River (Germany) and

kept in an Association for Assessment and Accreditation of Laboratory Animal Care (AAALAC) accredited facility with environmental control; 20–22°C, relative humidity 40%–60%, a 12-hour light–dark cycle (lights off at 6pm), housed in groups ($n=2/\text{cage}$) and given free access to standard rodent chow diet (A40, Safe, France) and water.

2.2 | Adeno-associated virus vectors and synthesis

AAV8 vector genome plasmids were generated to express human MARC1 (hMARC1) A165, hMARC1 165T or a control eGFP-2A-luciferase under the ApoE/hAAT1 promoter. This chimeric promoter contains the core promoter from the human alpha-1-antitrypsin (hAAT) gene and the enhancer/hepatic locus control region from the apolipoprotein E (ApoE) gene. The production of recombinant AAV was performed using the co-transfection of three plasmids into human embryonic kidney (HEK) 293T/17 cells (ATCC, CRL-11268) using Polyethyleneimine (PEI, PolySciences) reagent (DNA: PEI=1:2). The plasmids for transfection were at 1:1:1 weight ratio with the gene of interest, packaging (pAAV Rep-Cap, internal) and helper plasmid (TaKaRa, AAVpro system, 623066526655). HEK293T/17 cells were grown in DMEM (Gibco) containing 10% heat-inactivated fetal bovine serum (FBS), 100 U/mL penicillin and 100 µg/mL streptomycin.

Vectors were purified by ion-exchange chromatography using HiTrap SP HP column (1 mL, Cytiva, 29051324). Briefly, 293T/17 cells at 72h post transfection as described above were pelleted and sonicated with the pulse 1 second on and off at 35% amplitude, followed by Benzonase-based treatment (Merck). The treated cells were centrifuged to remove precipitated contaminants, and the supernatant was purified for AAV according to the manufacturer's instructions. The eluted AAV was concentrated using PES protein concentrators (100 KDa MWCO, Millipore) using formulation buffer containing glycerol and Plutonic® F-68 in Dulbecco's Phosphate Buffered Saline (D-PBS, Thermo Fisher).

The physical titre (genome copies/mL: GC/mL) of AAV vectors was measured by Digital Droplet Polymerase Chain Reaction (ddPCR) analysis with primers and a probe against inverted terminal repeats (ITRs). The following primers and probes were used for ddPCR. Universal ITR probe 5'-CACTCCCTCTCTGCGCGCTCG-3', forward primer 5'-GGAACCCCTAGTGATGGAGTT-3', and reverse primer 5'-CGGCCTCAGTGAGCGA-3'. The 5' end of the ITR probe was labelled with FAM. AAV capsid protein VP1, 2 and 3 were separated by sodium dodecyl sulfate-polyacrylamide gel electrophoresis (SDS-PAGE) and observed with InstantBlue™ Coomassie (Abcam, ab119211) staining to assess the purity of vector preparation.

2.3 | Hepatic overexpression of human mitochondrial amidoxime-reducing component 1 in mice

The mice ($n=4/\text{dose group}$) were given a tail vein injection (100 µL) of either PBS, AAV-eGFP-Luciferase (control), AAV-hMARC1 A165 or

AAV-hMARC1 165T at three dose levels: 1.0e10, 3.0e10 and 1.0e11 GC/mouse. Two weeks post dose, animals were anaesthetised with isoflurane and an orbital blood sample was taken with MultivetteR 600 K3E (Sarstedt) for plasma analysis of ALT, AST, total cholesterol and triglycerides. Liver tissue samples from the left lateral lobe were dissected and snap frozen in liquid nitrogen and stored at –80°C pending MARC1 mRNA and protein analyses.

2.4 | Hepatic mitochondrial amidoxime-reducing component 1 mRNA quantification

Liver tissue pieces were placed in a plastic tube containing a stainless-steel bead (Qiagen, 69989) and 900 µL of RLT buffer (Qiagen, 79216) and lysed for 2×2.5 minutes at 25 Hz using a tissue-lyser. RNA was subsequently purified using RNeasy Mini Kits (Qiagen, 74106). Isolated RNAs were reverse transcribed using the High-Capacity cDNA Synthesis kit (Applied Biosystems, 4368814), and gene expression was measured using real-time PCR with TaqMan Fast Advanced Master mix (Thermo Fisher, 4444556) on a Quantstudio 7 Flex Real-Time PCR machine (Applied Biosystems). The following TaqMan assays from Thermo Fisher were used: Hs00224227_m1 (*hMARC1*), Mm00725448_m1 (*mMarc1*) and Mm01315446_m1 (*mRplp0*; a.k.a. 36b4—used as internal normalization control).

2.5 | Hepatic mitochondrial amidoxime-reducing component 1 protein quantification

Liver tissue pieces (~50 mg) were placed in a 2 mL 96-well NUNC plate (Thermo Fisher, 278743) containing a stainless-steel bead (Qiagen, 69989) and 400 µL RIPA buffer containing a protease inhibitor cocktail (Thermo Fisher, 87785), and lysed for 2×1 minutes at 25 Hz using a tissue-lyser. Following centrifugation (20 min, 4000g). The supernatant was collected, and protein digestion was done according to the SP3 method.²¹ Digested peptides (2 µg/sample) were loaded onto Evtips and separated using an Evosep LC-system 8cm column in a 60 SPD gradient coupled to Thermo Scientific Lumos. The targeted peptides were as follows: GAEEMETVIPVDVMR (DJ1—used as internal normalization control), VHGLEIQGR (*mMarc1*), QLQVGTVSK (*mMarc2*) and VHGLEIEGR (*hMARC1*). Skyline Targeted Proteomics Environment (<http://skyline.maccosslab.org>) was used for identification and quantification of targeted peptides.

2.6 | Mitochondrial amidoxime-reducing component 1 overexpressing plasmids generation and site directed (in situ) mutagenesis

Human wild-type MARC1 A165 cDNA was synthesized and cloned in a pcDNA 3.1(+) vector with a V5-6XHis epitope tag at the C-terminus by GeneArt Gene Synthesis (Thermo Fisher Scientific). The

rs2642438 substitution was generated by site-directed mutagenesis introducing a single base-pair change in the wild-type *MARC1* gene sequence of the pcDNA3.1(+) plasmid (refer to [Supplementary Information](#)).

2.7 | In vitro treatments

In experimental conditions, the following inhibitors were used: Cycloheximide (200 µg/mL, 01810, Sigma-Aldrich) for protein synthesis inhibition; MG132 (15 µM, ab141003, Abcam) for inhibition of proteasomal degradation; Chloroquine (25 µM, C6628, Sigma-Aldrich) for lysosome-mediated protein degradation; and dibenzylquinazoline-2,4-diamine (DBEQ) (10 µM, SML0031, Sigma-Aldrich) for endoplasmic reticulum (ER)-associated degradation (ERAD) pathway inhibition, (Valosin-Containing Protein (VCP) inhibitor)²²; for inhibition of unfolded protein response pathways (UPR): IRE1 inhibitor—Toyocamycin (.3 µM, HY-103248, MedChemExpress)²³; ATF6 inhibitor—Ceapin-A7 (20 µM, HY-108434, MedChemExpress)²⁴; PERK inhibitor—GSK2606414 (.3 µM, HY-18072, MedChemExpress).²⁵

2.8 | Transient transfection

For transient overexpression, HuH-7 or HepG2 cells (cell culture details in suppl. Information) at 70% confluency were transfected using pcDNA3.1(+) with *MARC1* wild-type, or mutant forms to the final concentration of 2.5 µg/mL and Lipofectamine 3000 transfection reagent (L3000-075; ThermoFisher Scientific), following the manufacturer's protocol. An empty vector was always used as the negative control.

For genes downregulation, 24h after seeding and at 70% confluency, HepG2 cells were transiently transfected with SCR siRNA (AM4611; ThermoFisher Scientific), human *UBC* siRNA (28838; ThermoFisher Scientific), human *UBE2E1* siRNA (120313; ThermoFisher Scientific), human *UBE3EC* siRNA (21581; ThermoFisher Scientific) or human *MARC1* siRNA mixture (s34872, s34873, s34874; ThermoFisher Scientific) at 20 nM using Lipofectamine 3000 transfection reagent according to the manufacturer's protocol.

2.9 | Stable cell line generation

HepG2 cell lines stably overexpressing A165 or 165T *MARC1*-V5 were generated using the pcDNA3.1(+) expression vector containing *MARC1* A165 or *MARC1* 165T plasmid with a 6XHis-V5 epitope tag at the C-terminus of the target protein. An empty vector was used as a negative control. HepG2 cells were transfected using Lipofectamine 3000 reagent. Forty-eight hours post transfection, cells were diluted to 1:20 and seeded in a T150 flask, maintained in MEM media supplemented with 10% FBS, sodium pyruvate, L-glutamine, non-essential amino acids plus

500 µg/mL geneticin-G418 (stable cell media) to select resistant cells. At around 40% confluency, cells were collected and seeded in serial dilutions (1:4 to 1:8000) in a 96-well plate with stable cell media. Monoclonal colonies were gradually expanded. V5 expression levels were verified at each step by immunoblotting. *MARC1* mRNA was checked with real-time qPCR. The sequence was confirmed by Sanger sequencing.

2.10 | Immunoprecipitation

Cells stably overexpressing *MARC1* A165 or 165T were plated in 6-well plates and treated with MG132 (15 µM) for either 8 or 0 hours when they reached approximately 80% confluency. Following treatment, cells were chilled on ice, washed with PBS and lysed with RIPA lysis buffer (ab206996, Abcam) containing protease inhibitor. The lysate was incubated at 4°C for 30 minutes on a rotating shaker and then centrifuged at 10000g for 10 min at 4°C. The resulting supernatant was subjected to overnight incubation with anti-V5 magnetic beads (SAE0203, Sigma-Aldrich) on a rotating shaker at 4°C. The following day, the beads were washed three times with PBS, eluted using 2X-SDS-Laemmli buffer and saved for subsequent immunoblotting.

2.11 | Gene expression by quantitative polymerase chain reaction

For the in vitro studies, RNA from cells was extracted with RNeasy Plus mini kit (Qiagen) and retrotranscribed using high-capacity cDNA reverse transcription kit (4368813, Thermo Fisher Scientific) as per the manufacturer's protocol. Gene expression was assessed using three technical replicates by real-time qPCR using TaqMan probes [human *MARC1* (Hs00224227_m1), human *UBC* (Hs05002522_g1), human *UBE2E1* (Hs00979829), human *UBE3C* (Hs00904531_m1) and human *ACTB* (Hs01060665_g1)]. Data were analysed using the $2^{-\Delta\Delta C_t}$ method and normalized to the house keeping gene *ACTB*.

2.12 | Immunoblotting

The antibodies used were mouse anti-V5 (46-1157, Invitrogen—Life Technologies), rabbit anti-calnexin (C4731, Sigma-Aldrich), rabbit anti-ubiquitin (AB134953, Abcam), rabbit anti-K48-ubiquitin (ZRB2150, Sigma-Aldrich), rabbit anti-K63-ubiquitin (05-1308, Sigma-Aldrich), mouse anti-mitochondria (ab3298, Abcam) and rabbit anti-FACL4 (ab155282, Abcam). Blots were probed with primary antibodies, followed by the appropriate horseradish peroxidase (HRP)-conjugated secondary antibody (anti-mouse [NA931V, Abcam] anti-rabbit [NA934V, Abcam]), and then developed using ECL substrate (Immobilon Western Chemiluminescent HRP Substrate [Merck Millipore] or an ECL Western Blotting Detection System [GE Healthcare]). Immunoblot quantifications were performed using ImageLab Software (v 5.2.1).

2.13 | Subcellular fractionation

All the subcellular fractionation was performed using HepG2 cells stably overexpressing the MARC1-V5 A165 or 165T.

2.13.1 | Total membrane fractionation

The total membrane fractionation was performed as previously described.²⁶ Briefly, three confluent T150 flasks were collected in PBS, centrifuged and then lysed using Buffer A (50mM Tris-HCl, 250mM sucrose, with protease inhibitor at pH7.0) using 27-gauge needle for 15–20 times. After a brief centrifugation at 1000g for 1 min, supernatant was collected and ultracentrifuged at 100000g for 45 min. The pellet, containing membrane proteins, was then resuspended in 10mM Tris-HCl (pH7.4) and divided into equal volume for solubilization. All solvents for solubilization were added to the sample (1:1) and incubated for 1 h at 4°C and then ultracentrifuged at 100000g for 1 h at 4°C. The resulting pellets were resuspended in PBS and saved for immunoblotting.

2.13.2 | Mitochondria and mitochondria-associated membrane fractionation

Mitochondria-associated membrane (MAM) fractionation were performed by adapting the protocol already available.²⁷ Briefly, cells from 15 confluent T150 flasks of each A165 and 165T were collected using trypsinization and pooled. They were lysed in 8 mL sucrose homogenization media (.25 M sucrose, 10mM HEPES at pH 7.6 with protease inhibitor) using a 22G needle 15 times. Next, the lysate was centrifuged at 600g for 5 min, and the supernatant was collected and further centrifuged at 10300g for 10min at 4°C. The resulting pellet was resuspended in 300µL, loaded in percoll gradient (10mL 30% percoll v/v in 225mM mannitol, 25mM HEPES and .1mM EDTA) and ultracentrifuged at 95000g for 65min at 4°C. The upper white band containing the MAM fraction, and several thin lower white bands containing the mitochondrial fraction were collected, washed and further ultracentrifuged to obtain pure MAM and mitochondria fractions.

2.13.3 | Endoplasmic reticulum fraction

The ER was isolated with a discontinuous sucrose gradient as already described.^{11,14,27} The obtained ER fraction then underwent immunoblotting using anti-V5 to detect recombinant MARC1 and anti-calnexin as a marker for ER.

2.14 | Oil-Red-O staining

Oil-Red-O (ORO) staining was performed to evaluate intracellular neutral lipid content after MARC1 silencing. The total area for ORO

was determined as previously described.²⁸ HuH-7 cells were seeded in a coverslip at a density of 3×10^4 cells/well in 24-well plates and treated after 24 h with scramble siRNA or MARC1 siRNA at 20nM concentration. Forty-eight hours post-treatment, the cells were washed with PBS, with calcium and magnesium, and fixed with 2% paraformaldehyde (PFA) for 5 minutes. Intracellular lipids were stained with ORO solution (O0625, Sigma-Aldrich). Cell nuclei were stained with DAPI (D9542-5MG; Sigma-Aldrich). Slides were mounted with Dako Fluorescence-Mounting Medium (S3023, Agilent Technologies). Images were acquired using an Axio-KS-400 Imaging System and AxioVision 4.8 software (Zeiss) at 40x magnification. The ORO-stained area and the number of DAPI-stained nuclei were quantified using ImageJ (v. 1.52h, NIH). The obtained ORO-stained area was normalized to the number of DAPI-stained nuclei; data shown as ORO Area μm^2 /Nuclei.

2.15 | Statistics

All statistical analyses were performed using GraphPad Prism software. For in vivo studies, *p* values were calculated by one-way ANOVA with Tukey's multiple comparisons test and data are presented as mean \pm standard error of the mean (SEM).

For in vitro studies, *p* values were calculated by unpaired Student's *t*-test (all plots in Figures 2–4, Figure S2D–H) or by Mann-Whitney nonparametric test (Figure 6) and data are presented as mean values \pm standard deviation (SD) of at least three experiments unless specified otherwise.

3 | RESULTS

3.1 | Mitochondrial amidoxime-reducing component 1 165 threonine overexpression results in lower protein levels than 165 alanine in vivo and in vitro

To understand the effect of the alanine to threonine substitution at position 165 of MARC1, we overexpressed human MARC1 A165 or MARC1 165T in mice liver using recombinant adeno-associated viruses (AAVs) at three different dose levels (1e10, 3e10 and 1e11 GC/mouse), and compared the effects to PBS and AAV control groups (Figure 1). Hepatic MARC1 mRNA expression levels increased dose-dependently following rAAV-hMARC1 A165 and 165T administration and at the highest dose level, overexpression of 165T tended to result in higher MARC1 mRNA levels compared to A165 (Figure 1A). However, when assessing hepatic protein levels of MARC1 using targeted mass-spectrometry, overexpression of MARC1 165T resulted in lower protein levels compared to MARC1 A165 at the middle and high AAV dose (Figure 1B). Mouse *Marc1* protein levels, mouse *Marc1* mRNA levels, body weight, spleen weight and plasma levels of ALT, AST, cholesterol and triglycerides were not affected by rAAV-MARC1 A165 and 165T administration (Figure 1C and Figure S1). In

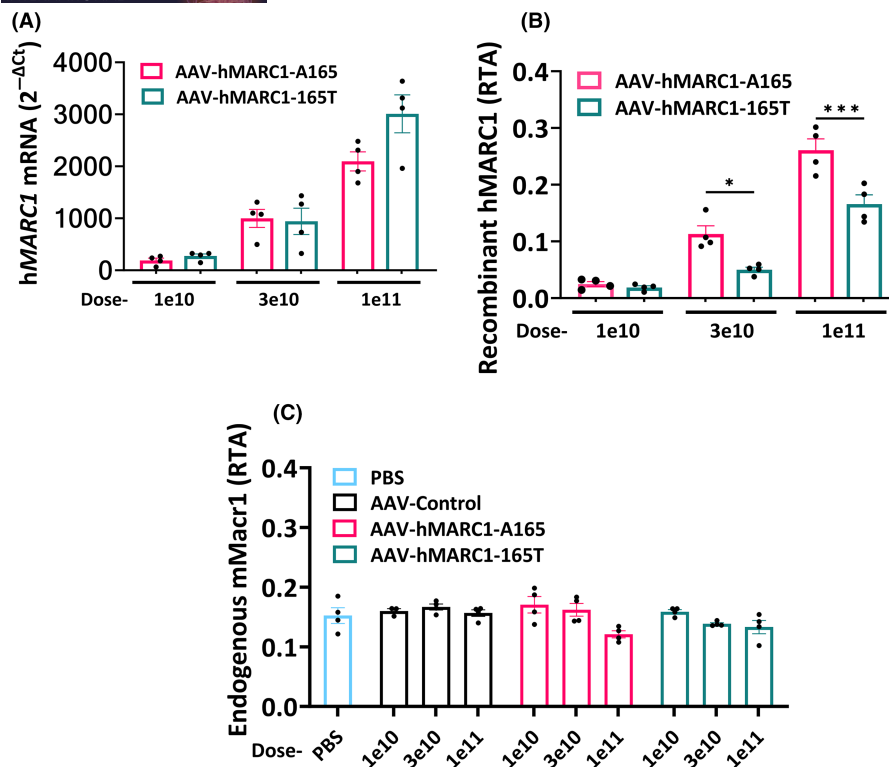


FIGURE 1 Hepatic overexpression of human MARC1 165T leads to lower protein levels compared to overexpression of human MARC1 A165 in mice. Female C57Bl/6N mice were injected with either PBS, recombinant AAV control, AAV-hMARC1 A165 or AAV-hMARC1 165T at three dose levels, 1.0E10, 3.0E10 and 1.0E11 GC/mouse, and sacrificed 2 weeks post injection. (A) qPCR analysis of human MARC1 mRNA expression in the liver. MS targeted proteomics analysis of (B) human (AAV-induced) MARC1 protein and (C) mouse (endogenous) Marc1 protein abundance in the liver. Data presented as mean \pm SEM ($n=4$ /dose group). * $p<.05$; *** $p<.001$ by one-way ANOVA with Tukey's multiple comparisons test. hMARC1, recombinant human MARC1 protein; mMacr1, endogenous mouse Marc1 protein; RTA, relative total abundance.

summary, the hMARC1 165T genetic variant is associated with reduced hepatic MARC1 protein levels in vivo in mice. To confirm the in vivo results, we acutely overexpressed MARC1 A165 wild-type or 165T mutant proteins tagged with a V5 at the C terminus in two different hepatocyte cell lines, namely HepG2 and HuH-7. To ensure specificity, we consistently assessed the levels of recombinant MARC1 protein by using a V5 antibody.

Consistent with the in vivo data, overexpression of MARC1 165T-V5 resulted in lower levels of protein as compared to the A165-V5 wild-type in both cell lines (Figure S2A,B,D,E), despite higher amount of mRNA level of the 165T variant (Figure S2G,H).

Following this, we acutely overexpressed MARC1-V5 A165 and 165T in MARC1 knockout HepG2 cells that are homozygous for the wild-type MARC1, that is, A165. MARC1 RNA levels were similar in these knock out cells as compared to wild-type cells indicating that endogenous MARC1 does not affect the acute MARC1-V5 overexpression (Figure S2J).

3.2 | Mitochondrial amidoxime-reducing component 1 p.Ala165 is required for protein stability

To understand whether the alanine at position 165 is required for protein stability, we substituted the MARC1 A165 amino acid with

several alternative amino acids or with a deletion. Specifically, we deleted the alanine in position 165 of the protein, or changed it into: glycine, the smallest amino acid, proline an amino acid hindering alpha helix, serine the closest amino acid to threonine, valine, the closest amino acid to alanine, tryptophan the largest amino acid, tyrosine an amino acid with a phenyl group and overexpressed these mutant proteins in HepG2 and HuH-7 cells. Overexpression of these mutants showed that, irrespective of the aminoacidic change or deletion, all the mutations resulted in lower levels of MARC1 (Figure 2A,B) despite similar mRNA levels (Figure S2K,L). These data suggest that Alanine 165 is required for maintaining protein levels.

3.3 | Mitochondrial amidoxime-reducing component 1 p.165Thr intracellular degradation is accelerated through the proteasome

To understand the mechanism underlying lower protein levels observed with the 165T protein, we generated HepG2 cells stably overexpressing the MARC1 A165-V5 or 165T-V5 tagged proteins. Stable overexpressing cells significantly recapitulated the phenotype of the acute overexpression (Figure S2C,F,I). Next, we incubated these cells with cycloheximide, an inhibitor of protein synthesis, for 8 h and measured the protein levels. We detected reduced MARC1

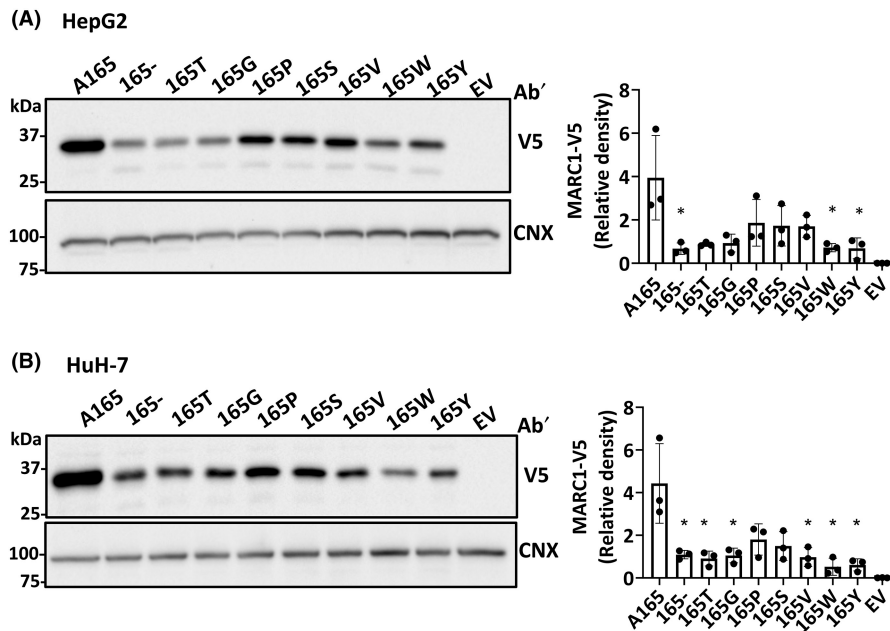


FIGURE 2 Alanine at 165 is required for MARC1 protein stability. Acute overexpression of MARC1-V5 A165 wild-type or 165-, 165T, 165G, 165P, 165S, 165V, 165W and 165Y mutants in (A) HepG2 and (B) HuH-7 cells. Forty-eight hours after transfection, cells were lysed, and equal volume of total proteins was loaded into 10% SDS-PAGE and immunoblotted against V5 and Calnexin (CNX) antibodies. The intensity of the western blotting bands was measured by Image Lab Software (Bio-Rad), normalized to calnexin and expressed as relative density. Transfection with the empty vector was used as control. Data presented as mean \pm SD ($n=3$). * $p < .05$ by unpaired t -test comparing each mutant to the wild-type (A165). 165-, Deletion; 165T, Threonine (mutant and protective allele); 165G, Glycine; 165P, Proline; 165S, Serine; 165V, Valine; 165W, Tryptophan; 165Y, Tyrosine; A165, Alanine (wild-type and risk-allele); EV, empty vector.

165T-V5 mutant protein levels after incubation with cycloheximide (200 μ g/mL) and no differences in the A165-V5 wild-type protein levels (Figure 3A and Figure S3A). These data suggest that MARC1 165T-V5 lower levels are due to higher protein degradation. To formally test this hypothesis, we incubated MARC1 A165-V5 and 165T-V5 stable cells with MG132, a proteasome inhibitor, for 8 hours and measured the protein levels. After incubation with 15 μ M MG132, we detected a five-fold increase in the levels of the 165T-V5 while the levels of A165-V5 were only doubled at best (Figure 3B and Figure S3B). These data suggest that MARC1 165T-V5 lower levels are due to higher proteasomal degradation. To test whether this was due to ubiquitin-mediated proteasomal degradation, we down-regulated ubiquitin C (*UBC*), ubiquitin conjugating enzyme E2-E1 (*UBE2E1*) and ubiquitin protein ligase E3C (*UBE3C*), the key genes encoding proteins initiating ubiquitin-mediated proteasomal degradation. Downregulation of these genes resulted in rescuing the phenotype, namely restoring the 165T mutant protein levels to the same level of A165 wild-type protein (Figure 3C).

To further confirm these data, we examined polyubiquitination of MARC1 A165-V5 and 165T-V5 by immunoprecipitation with V5 antibody, after incubation with MG132. We observed that 165T exhibited higher levels of polyubiquitination after incubation with the proteasome inhibitor than the A165 (Figure 3D).

Proteins to be redirected to the proteasome for degradation are linked to the lysine-48 residue of ubiquitin. To understand whether the lysine-48 of ubiquitin is bound to MARC1, we incubated cells with MG132 for 8 hours, immunoprecipitated with a V5 antibody and

then measured levels of this protein by immunoblotting with an antibody specific for ubiquitin lysine-48. We found that MARC1 165T exhibited higher levels of lysine-48 ubiquitination compared to A165 (Figure 3E). These data demonstrate that 165T is more degraded by the proteasome due to higher lysine-48 ubiquitination. Finally, immunoblotting with an antibody specific for lysine-63, which targets proteins for translocation, and regulates protein interactions,²⁹ revealed no differences between A165 and 165T (Figure 3F).

3.4 | Lysosomal mediated and endoplasmic reticulum degradation pathways are not involved in mitochondrial amidoxime-reducing component 1 p.165Thr degradation

In addition to the ubiquitin-proteasome system, there are other pathways for intracellular protein degradation.^{30,31} Among these, we investigated the endoplasmic reticulum-associated protein degradation (ERAD) and the lysosomal-mediated protein degradation pathway.

To explore potential differences between the A165 and 165T proteins in the ERAD pathway, we incubated A165-V5 and 165T-V5 cells with dibenzylquinazoline-2,4-diamine (DBEq), for 8 hours and measured MARC1 protein levels. DBeQ (10 μ M) is an ERAD pathway inhibitor that selectively reduces p97 ATPase activity. After inhibition of the ERAD pathway, there was no difference in the degradation pattern between the A165 and 165T proteins (Figure 4A and Figure S3C).

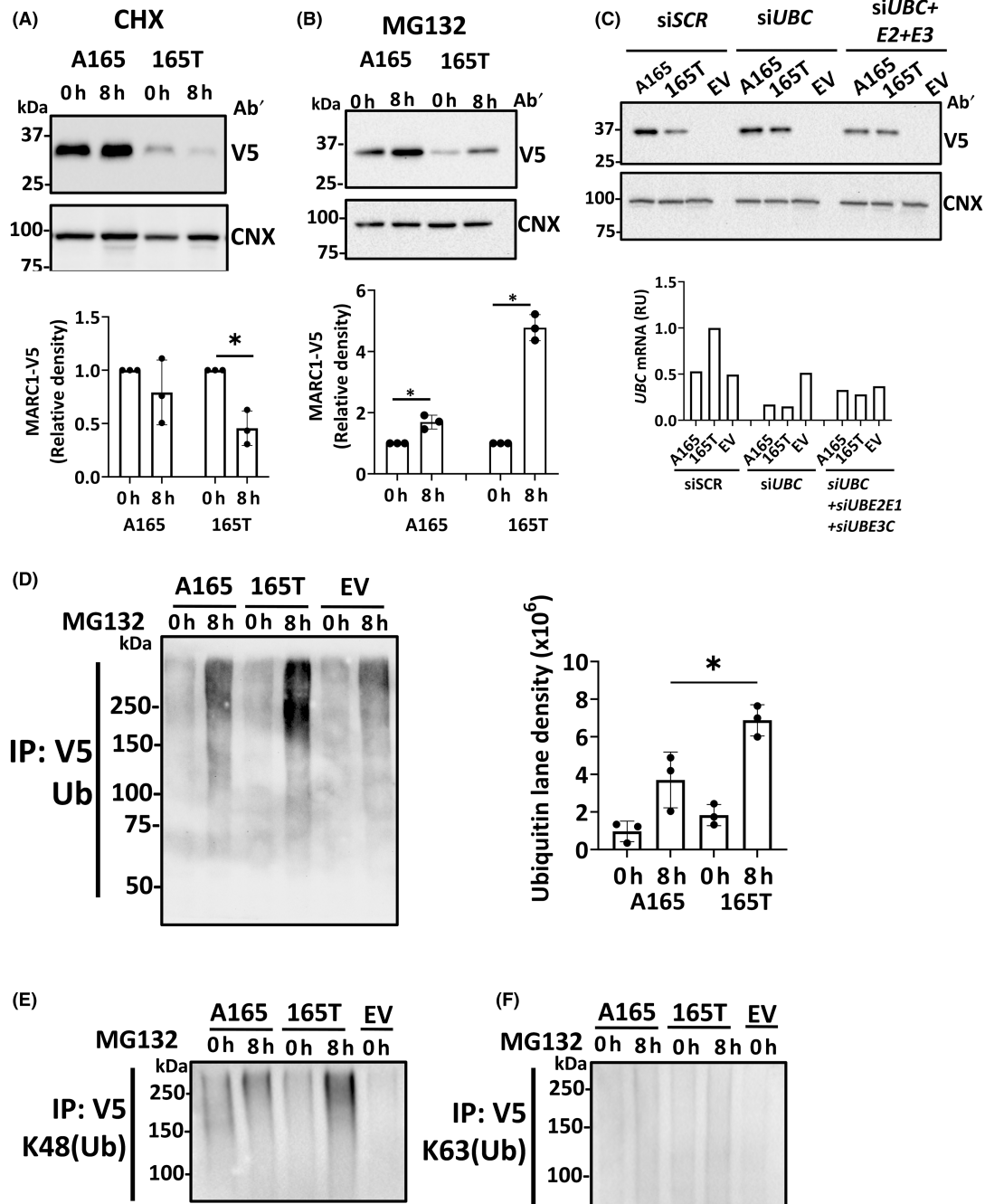


FIGURE 3 MARC1 165T shows increased degradation by the ubiquitin-proteasome pathway compared to A165. MARC1-V5 A165 and 165T protein level in HepG2 stable cell lines at baseline and 8h after incubation with (A) cycloheximide (CHX, inhibitor of protein synthesis) or (B) MG132 (inhibitor of proteasome). When at 70% confluency, cells were incubated with 200 μ g/mL cycloheximide or with 15 μ M of MG132 for 8h. Then, both cells at baseline and cells 8h after incubation were lysed; an equal volume of total proteins was loaded into 12% SDS-PAGE and immunoblotted against V5 and Calnexin (CNX) antibodies. The intensity of the western blotting bands was measured by Image Lab Software (Bio-Rad), normalized to calnexin and expressed as relative density. Protein levels were presented as relative to baseline values. MARC1-V5 A165 and 165T protein level in HepG2 stable cell lines transfected with scramble-siRNA (siSCR), siRNA for ubiquitin C (siUBC), or a combination of 3 siRNAs, that is, UBC, UBE2E1 and UBE3C (siUBC + E2 + E3), key-role players in the ubiquitination process (C). Cells stably transfected with the empty vector were used as control. Forty-eight hours after transfection, cells were harvested and processed for both qPCR and immunoblotting on 12% SDS-PAGE. To understand the ubiquitination of MARC1, stable cells (A165, 165T or negative control empty vector) were immunoprecipitated using V5-magnetic beads using RIPA buffer to only get ubiquitin from MARC1 and not from any other interacting partners (D). MG132 was added in samples to reduce proteasomal degradation of MARC1. Samples were eluted using 2X SDS-Laemmli buffer, loaded on 8% SDS-PAGE and ran 2.5h to include highly polyubiquitinated MARC1. Then, they were immunoblotted against ubiquitin antibody. For the quantification of ubiquitin; the whole lane was quantified and presented as relative to MARC1 overexpressing cells. The smear in EV is the non-specific background. (E and F) Immunoblot of K48-linked ubiquitin; or K63-linked ubiquitin after immunoprecipitation. Samples were loaded on 8% SDS-PAGE. Data presented as mean and SD ($n=3$). p values calculated by unpaired t -test. * $p < .05$.

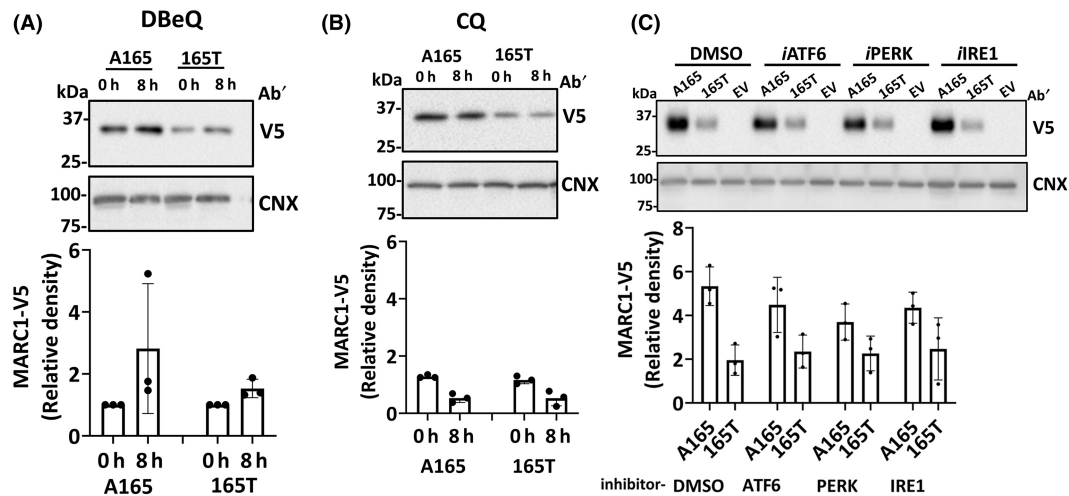


FIGURE 4 No difference in endoplasmic reticulum (ER) degradation pathways and in lysosomal degradation between MARC1 A165-V5 and 165T-V5. MARC1-V5 A165 and 165T protein level in HepG2 stable cell lines at baseline and 8h after incubation with (A) ER associated degradation pathway (p97/VCP) inhibitor, DBEq (10 μ M) or (B) Chloroquine (CQ), lysosomal pathway inhibitor. Upon 70% confluency, cells were incubated with 10 μ M DBEq or with 25 μ M CQ for 8h. Then, both cells at baseline and cells 8h after incubation were lysed; an equal volume of total proteins was loaded into 12% SDS-PAGE and immunoblotted against V5 and Calnexin (CNX) antibodies. The intensity of the western blotting bands was measured by Image Lab Software (Bio-Rad), normalized to calnexin and expressed as relative density. Protein levels are presented relative to baseline values. (C) Upon 70% confluency, MARC1-V5 A165 or 165T overexpressing stable cell lines at baseline and 4h after incubation with either DMSO (vehicle control), ATF6 inhibitor (iATF6, 20 μ M Ceapin-A7), PERK inhibitor (iPERK, .3 μ M GSK2606414) or IRE1 inhibitor (iIRE1, .3 μ M Toyocamycin) were lysed. An equal volume of total protein was loaded into 12% SDS-PAGE and immunoblotted against V5 and Calnexin (CNX) antibodies. The intensity of the western blotting bands was measured by Image Lab Software (Bio-Rad), normalized to calnexin and expressed as relative density. Data presented as mean and SD ($n=3$). p values calculated by unpaired t -test.

Next, to inhibit the lysosomal-mediated protein degradation pathway, we incubated cells with (CQ, 25 μ M) for 8 hours. CQ inhibits autophagy by impairing autophagosome fusion with lysosomes. After inhibition of the lysosome degradation pathway, there was no difference in the degradation between the A165 and 165T proteins (Figure 4B and Figure S3D).

We also investigated if the MARC1 wild-type and mutant protein would be degraded via the unfolded protein response (UPR). We incubated A165-V5 and 165T-V5 cells for 4 hours with the inhibitors of the UPR pathways (20 μ M Ceapin-A7 or .3 μ M GSK2606414 or .3 μ M Toyocamycin, along with a vehicle control, DMSO). Ceapin-A7 is a selective blocker of ATF6, GSK2606414 is a cell-permeable protein kinase R-like endoplasmic reticulum (ER) kinase (PERK) inhibitor, and Toyocamycin is an adenosine analogue acting as an XBP1 inhibitor that affects IRE1 auto-phosphorylation. After inhibition of the UPR pathway, no difference in the protein levels was observed between A165 and 165T (Figure 4C).

These findings suggest that the 165T substitution does not affect protein degradation by influencing ERAD, lysosome-mediated protein degradation and the UPR pathway.

3.5 | Mitochondrial amidoxime-reducing component 1 is localized in endoplasmic reticulum, mitochondria and mitochondria-associated membrane

To assess whether the protein-membrane interaction was affected by the MARC1 A165T substitution, we incubated the total membrane fraction from HepG2 cells stably overexpressing the 165T-V5

or A165-V5 protein with different solubilizing buffers. We found that MARC1 A165 and 165T were dissociated from the membrane fraction by the detergents, Triton X-100 and SDS, and not by incubation with 1 M NaCl or .2 M Na_2CO_3 . In line with previous studies,^{20,32} these data show that MARC1 is attached to endomembranes and are thus consistent with the notion of MARC1 being an integral membrane protein. Moreover, there were no differences in regard to membrane dissociation between the wild-type and mutant proteins (Figure 5A).

To confirm the intracellular localization of MARC1 and to determine whether the amino acid change induces protein mislocalization, we purified the endoplasmic reticulum, mitochondria and MAM fractions from cells stably overexpressing the A165-V5 or 165T protein. We found that both MARC1 A165 and 165T co-localized with mitochondria, MAM fraction and ER fraction with no changes detected between A165 or 165T (Figure 5B,C). These data show that MARC1 is attached to endomembranes and that the 165T variant does not result in membrane displacement.

3.6 | Mitochondrial amidoxime-reducing component 1 downregulation decreases intracellular fat content in human hepatoma cells

To test whether hepatic downregulation of MARC1 affects the intracellular fat content, we silenced MARC1 in HuH-7 cells cultured in 2D (HuH-7 cells are homozygous for the MARC1 wild-type variant, A165), followed by Oil-Red-O staining. The silencing efficiency of

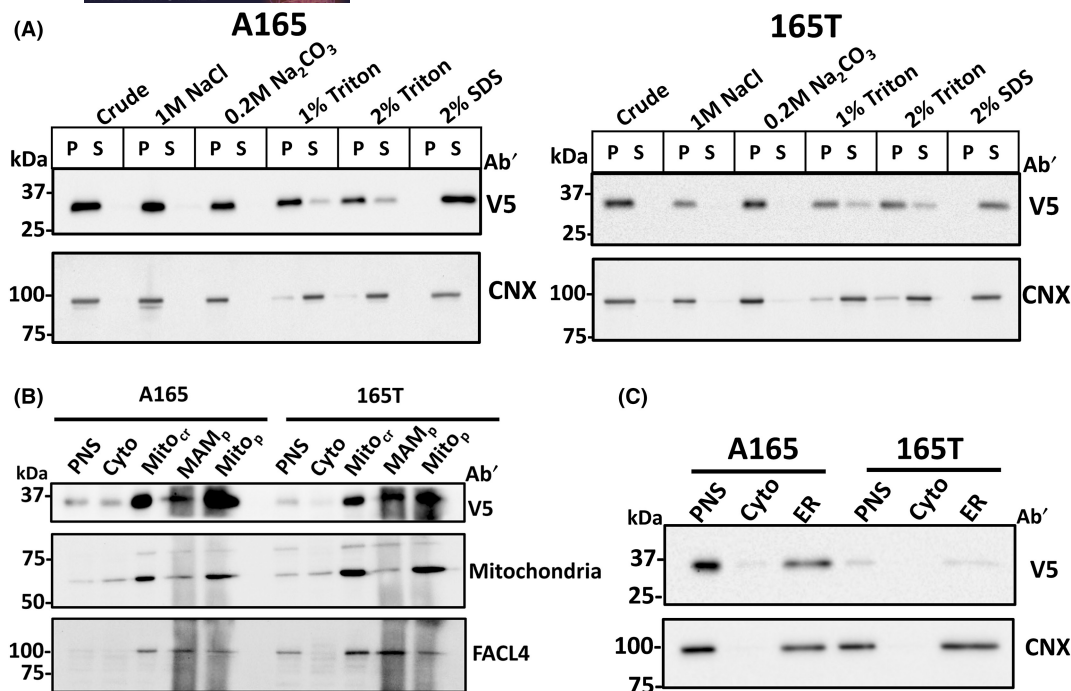


FIGURE 5 MARC1 is localized in endomembranes, and there is no difference between the 165T and A165 in terms of localization. (A) Total membrane fractionation and solubilization: 3 confluent T150 flasks for each of A165 and 165T MARC1-V5 overexpressing stable cells were processed for total membrane fractionation and followed by solubilization in different conditions. In the crude total membrane fraction, pellet (P) contains all the membrane proteins and supernatant (S) contains cytosolic proteins. The crude protein is then incubated with high salt concentration (1M NaCl) to separate peripheral membrane proteins from integral proteins; .2M Na₂CO₃ to break protein-protein interactions without disrupting membranes; mild and denaturing detergents respectively (1% Triton-X, 2% triton-X and 2% SDS). After incubating with solvents, pellet (P) contains the proteins still in the membrane and supernatant (S) fractions contain the displaced proteins from membrane. Calnexin (CNX) is an integral membrane protein and blotted as an internal control. (B) Mitochondrial and MAM fractionation: 15 confluent T150 flasks of each A165 and 165T were used for MAM and mitochondrial fractionation. Cyto, cytosolic fraction; MAM_p, pure mitochondria-associated membrane fraction; Mito_{cr}, crude mitochondria; Mito_p, pure mitochondria; PNS, post nuclear supernatant. Sample ran in 12% SDS-PAGE, blotted against a mitochondria antibody (60kDa pyruvate dehydrogenase multienzyme complex (PDC-E2) subunit as a marker for Mitochondria; FACL4 is a marker for mitochondria-associated membrane (MAM). (C) ER fractionation: 2T150 confluent flasks were used to isolate ER fraction. Samples were run in 12% SDS-PAGE. Calnexin (CNX) was used as the ER marker. Cyto, cytosolic fractions; ER, endoplasmic reticulum fractions; PNS, post nuclear supernatant.

MARC1 downregulation was >90%, resulting in ~50% reduction of intracellular lipids (Figure 6).

4 | DISCUSSION

The main finding of this work is that the alanine to threonine substitution at position 165 of MARC1 results in a hypomorphic variant of the protein. This is mediated by proteasomal degradation of the MARC1 protein due to higher lysine-48 ubiquitination in 165T. Moreover, we found that the aminoacidic change does not affect the protein localization in endomembranes.

Using a liver specific and stable overexpression system in mice, overexpression of human MARC1 165T mutant resulted in lower hepatic protein levels as compared to the A165 wild-type despite similar mRNA levels, indicating a post translational mechanism. This overexpression did not change the endogenous murine Marc1 protein levels and did not affect mouse body weight, liver transaminases or plasma lipid levels.

We recapitulated the *in vivo* data in two human hepatoma cell lines and generated a series of MARC1 variants at position 165: (a) testing whether the size and nature of the amino acid would be necessary for the deleterious effect by substituting A165 with threonine, serine, tryptophan and tyrosine (b) the predicted crystal structure of MARC1 indicates the 165-alanine residue is located within an alpha helix domain²⁰ and thus we created *in situ* mutants that potentially disrupt alpha helix, that is, proline, known to break alpha helix, glycine, the smallest amino acid not favouring alpha helix formation and (c) we hypothesized that by using valine the most similar amino acid to alanine, or by ablating the amino acid at position 165, we would rescue the phenotype by restoring protein levels. Notably, overexpression of all the mutants irrespective of the change resulted in similarly low amount of MARC1 proteins indicating that 165 Alanine is required at that position for protein stability.

Given that the protein level was lower in 165T compared to A165, despite higher mRNA expression, we hypothesized that the aminoacidic change would result in lower protein stability. Indeed, when cells were incubated with cycloheximide, an inhibitor of the

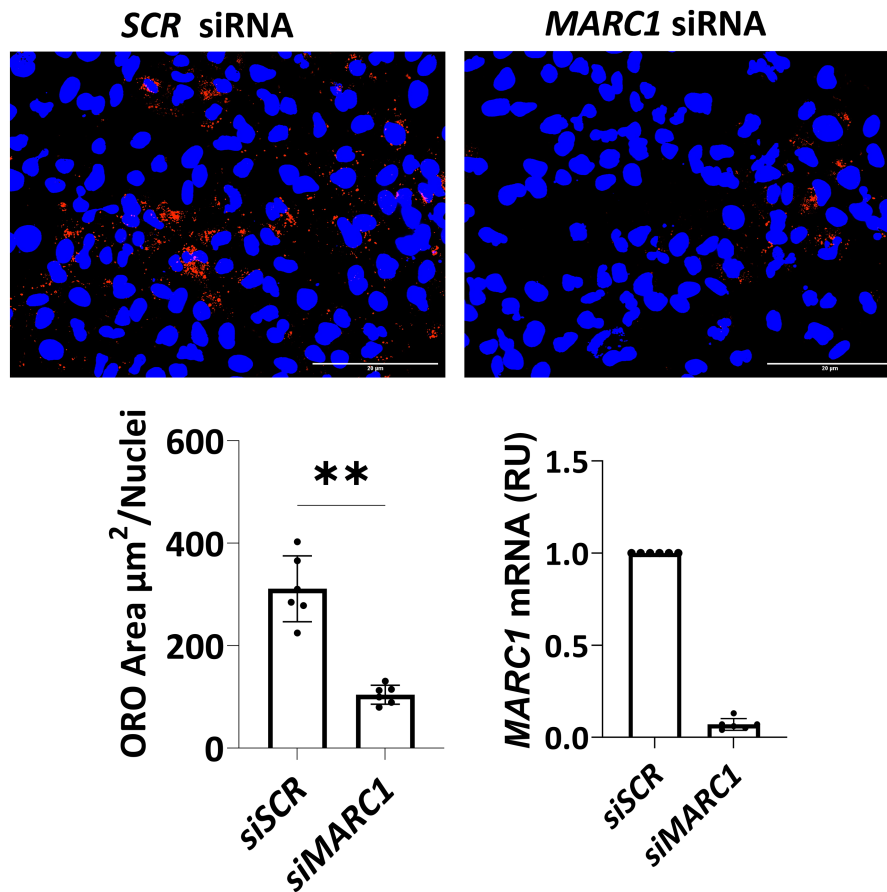


FIGURE 6 MARC1 downregulation decreases intracellular fat content in human hepatoma cells. HuH-7 cells were seeded in 24-well plates (3×10^4 cells/well) with DMEM low glucose 10% FBS and treated after 24h with scramble siRNA or MARC1 siRNA 20nM. Cells were stained with DAPI and Oil-Red-O (ORO) and visualized under Axio KS 400 Imaging System (Zeiss) at 40x magnification, acquired using AxioVision v4.8 software (scale bar 20µm). ORO (red channel) was captured in Texasred. Each experiment had on average 12 images, taken in the same acquisition settings. Data shown as average of 6 independent experiments (\pm SD), with the total ORO area divided by the number of nuclei in the field. The p value was calculated by Mann-Whitney nonparametric test. $**p < .01$. MARC1 downregulation efficiency in 6 respective experiments as shown in qPCR results.

cellular protein synthesis, we observed a higher decay of the 165T protein over time as compared to the A165, indicating accelerated degradation. Protein degradation in cells is in large mediated via four different pathways, namely ubiquitin-mediated proteasomal degradation (UPS), endoplasmic reticulum-associated degradation (ERAD), lysosomal degradation and unfolded protein response (UPR).³¹ In the present study, we show that MARC1 A165 protein is degraded through the proteasomal pathway, with MARC1 165T mutant protein being polyubiquitinated to a larger extent and thus degraded faster. We also show that the higher proteasomal degradation of 165T is mediated by lysine-48 ubiquitination.

Overall, our results support the notion that the MARC1 alanine to threonine substitution at position 165 of the protein results in a hypomorphic variant due to enhanced protein degradation (Figure 7). Consistent with this model, carriers of the minor allele of a nonsense mutation in MARC1 (p.LOF 200Ter) have lower transaminase levels and reduced risk of cirrhosis.¹⁵

MARC1 is a protein located in endomembranes and in mitochondria and we tested whether the aminoacidic change may

result in a displacement of MARC1 from these membranes. To test this hypothesis, we examined total membrane fractionations from cells stably overexpressing either the wild-type or mutant protein and solubilized the protein using different salts and detergents. We observed that the MARC1 A165 wild-type and 165T mutant were dissociated upon addition of the detergents Triton X-100 or Sodium dodecyl sulphate, indicating that this is an integral membrane protein. However, we did not find any differences between A165 wild-type and 165T mutant with regard to strength of the protein interaction with membranes and its subcellular localization.

Given our findings that the alanine to threonine substitution at 165 results in a hypomorphic variant of the MARC1 protein, that is, reduced protein levels, and since this variant is associated with a protection from MASLD, we assessed intracellular fat content in the HuH-7 cell line upon silencing of endogenous MARC1 mRNA expression. Consistently, the intracellular lipid content was reduced after downregulation of MARC1, indicating that the alanine substitution to a threonine at position 165 contributes to protection against

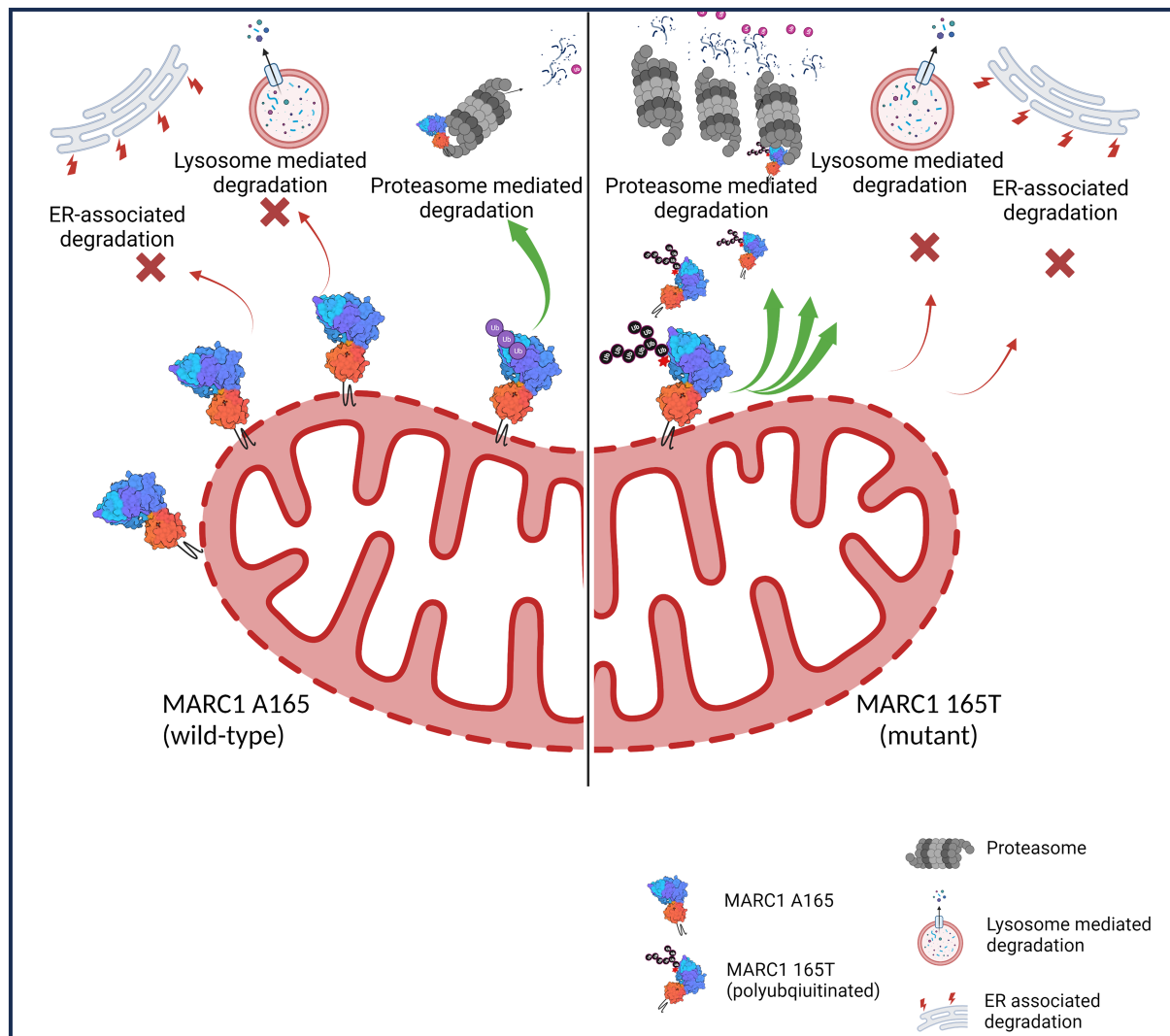


FIGURE 7 Amino acid substitution at A165T in MARC1 reduces protein stability by inducing ubiquitin–proteasome pathway. Figure was created with [BioRender.com](https://www.biorender.com).

liver diseases by reducing MARC1 protein levels. However, we did not measure intracellular lipid levels after downregulating MARC1 in human primary hepatocytes.

Limitation of our study is that we did not examine whether the aminoacidic substitution affects MARC1 enzymatic activity. Future studies with purified enzymatic protein are warranted to answer this question. However, previous studies indicate that MARC1 A165 and 165T may have similar MOCO binding and enzymatic activity^{20,32–34} Another limitation is that we did not elucidate the physiological role of MARC1 in hepatocyte triglyceride homeostasis and if MARC1 inactivation may affect triglyceride synthesis, beta-oxidation or very low-density lipoprotein secretion.

In conclusion, the alanine at position 165 of MARC1 is required for protein stability and its Threonine substitution results in a hypomorphic variant. Collectively, the data support the notion that downregulation of MARC1 will be an effective therapeutic strategy to reduce MASLD and ALD. However, future studies will be needed

to translate these results in humans and to understand whether this strategy may be effective only in carriers of the MARC1 A165 wild-type or also 165T mutant protein carriers.

AUTHOR CONTRIBUTIONS

Conceptualization and funding acquisition: SR. Investigation: TD, EC, GP, FRN, TK, AL, YD, MP, SW and DL. Methodology: TD, TK, YD, DL and SR. Software: TD, KS, EC and GP. Supervision: DL and SR. Data interpretation: TD, KS, EC, GP, RMM, TK, DL and SR. Visualization: TD, KS, EC, FRN, LK, TK and DL. Writing—original draft: TD, SR, AL, KS, EC, GP, LK, TK, YD, MP, SW, DL, RMM and FRN. Writing—review and editing: TD, SR, AL, KS, EC, GP, LK, TK, YD, MP, SW, DL, RMM and FRN.

ACKNOWLEDGEMENTS

We would like to thank the staff at the AstraZeneca laboratory animal science department for help with the experiments.

FUNDING INFORMATION

This research was funded by the Swedish Cancerfonden (22 2270 Pj), the Swedish Research Council (Vetenskapsradet (VR), 2023-02079), the Swedish state under the Agreement between the Swedish government and the county councils (the ALF agreement, ALFGBG-965360), the Swedish Heart Lung Foundation (20220334), the Wallenberg Academy Fellows from the Knut and Alice Wallenberg Foundation (KAW 2017.0203), the Novonordisk Distinguished Investigator Grant—Endocrinology and Metabolism (NNF23OC0082114), the Novonordisk Project grants in Endocrinology and Metabolism (NNF20OC0063883), AstraZeneca Agreement for Research, and AstraZeneca Cosolve.

CONFLICT OF INTEREST STATEMENT

SR is a consultant for AstraZeneca and received research grant for working on the molecular genetics of steatotic liver disease. SR consulted for Ribocure AB, Foresite Laboratory, Sanofi-Aventis, AMGEN, Novartis and Wave Life Sciences. TK, AL, YD, MP, SW and DL are AstraZeneca employees.

DATA AVAILABILITY STATEMENT

All data can be found in the main text or the supplementary materials. Any additional data not covered here can be requested directly from the authors.

ORCID

Tanmoy Dutta  <https://orcid.org/0000-0003-2816-2899>

Rosellina M. Mancina  <https://orcid.org/0000-0002-1126-3071>

Stefano Romeo  <https://orcid.org/0000-0001-9168-4898>

REFERENCES

- Valenti L, Aghemo A, Forner A, Petta S, Romeo S, Nahon P. Measuring the impact of the updated Steatotic liver disease nomenclature and definition. *Liver Int.* 2023;43(11):2340-2342. doi:10.1111/liv.15731
- Huang DQ, El-Serag HB, Loomba R. Global epidemiology of NAFLD-related HCC: trends, predictions, risk factors and prevention. *Nat Rev Gastroenterol Hepatol.* 2021;18(4):223-238. doi:10.1038/s41575-020-00381-6
- Rinella ME, Lazarus JV, Ratzliff V, et al. A multi-society Delphi consensus statement on new fatty liver disease nomenclature. *Hepatology.* 2023;78(6):1966-1986. doi:10.1097/HEP.0000000000000520
- Younossi ZM, Golabi P, Paik JM, Henry A, Van Dongen C, Henry L. The global epidemiology of nonalcoholic fatty liver disease (NAFLD) and nonalcoholic steatohepatitis (NASH): a systematic review. *Hepatology.* 2023;77(4):1335-1347.
- Fernando DH, Forbes JM, Angus PW, Herath CB. Development and progression of non-alcoholic fatty liver disease: the role of advanced glycation end products. *Int J Mol Sci.* 2019;20(20):5037. doi:10.3390/ijms20205037
- Pelusi S, Valenti L. Hepatic fat as clinical outcome and therapeutic target for nonalcoholic fatty liver disease. *Liver Int.* 2019;39(2):250-256. doi:10.1111/liv.13972
- Dongiovanni P, Stender S, Pietrelli A, et al. Causal relationship of hepatic fat with liver damage and insulin resistance in nonalcoholic fatty liver. *J Intern Med.* 2018;283(4):356-370. doi:10.1111/joim.12719
- Dongiovanni P, Petta S, Mannisto V, et al. Statin use and non-alcoholic steatohepatitis in at risk individuals. *J Hepatol.* 2015;63(3):705-712. doi:10.1016/j.jhep.2015.05.006
- Romeo S, Kozlitina J, Xing C, et al. Genetic variation in PNPLA3 confers susceptibility to nonalcoholic fatty liver disease. *Nat Genet.* 2008;40(12):1461-1465. doi:10.1038/ng.257
- Sookoian S, Pirola CJ. Meta-analysis of the influence of I148M variant of patatin-like phospholipase domain containing 3 gene (PNPLA3) on the susceptibility and histological severity of non-alcoholic fatty liver disease. *Hepatology.* 2011;53(6):1883-1894. doi:10.1002/hep.24283
- Pirazzi C, Adiels M, Burza MA, et al. Patatin-like phospholipase domain-containing 3 (PNPLA3) I148M (rs738409) affects hepatic VLDL secretion in humans and in vitro. *J Hepatol.* 2012;57(6):1276-1282. doi:10.1016/j.jhep.2012.07.030
- Kozlitina J, Smagris E, Stender S, et al. Exome-wide association study identifies a TM6SF2 variant that confers susceptibility to nonalcoholic fatty liver disease. *Nat Genet.* 2014;46(4):352-356. doi:10.1038/ng.2901
- Speliotes EK, Yerges-Armstrong LM, Wu J, et al. Genome-wide association analysis identifies variants associated with nonalcoholic fatty liver disease that have distinct effects on metabolic traits. *PLoS Genet.* 2011;7(3):e1001324. doi:10.1371/journal.pgen.1001324
- Mancina RM, Dongiovanni P, Petta S, et al. The MBOAT7-TMC4 variant rs641738 increases risk of nonalcoholic fatty liver disease in individuals of European descent. *Gastroenterology.* 2016;150(5):1219-1230.e6. doi:10.1053/j.gastro.2016.01.032
- Emdin CA, Haas ME, Khera AV, et al. A missense variant in mitochondrial Amidoxime reducing component 1 gene and protection against liver disease. *PLoS Genet.* 2020;16(4):e1008629.
- Jamialahmadi O, Mancina RM, Ciociola E, et al. Exome-wide association study on alanine aminotransferase identifies sequence variants in the GPAM and APOE associated with fatty liver disease. *Gastroenterology.* 2021;160(5):1634-1646.e7. doi:10.1053/j.gastro.2020.12.023
- Luukkonen PK, Juuti A, Sammalkorpi H, et al. MARC1 variant rs2642438 increases hepatic phosphatidylcholines and decreases severity of non-alcoholic fatty liver disease in humans. *J Hepatol.* 2020;73(3):725-726. doi:10.1016/j.jhep.2020.04.021
- Innes H, Buch S, Hutchinson S, et al. Genome-wide association study for alcohol-related cirrhosis identifies risk loci in MARC1 and HNRNPUL1. *Gastroenterology.* 2020;159(4):1276-1289.e7. doi:10.1053/j.gastro.2020.06.014
- Klein JM, Busch JD, Potting C, Baker MJ, Langer T, Schwarz G. The mitochondrial amidoxime-reducing component (mARC1) is a novel signal-anchored protein of the outer mitochondrial membrane. *J Biol Chem.* 2012;287(51):42795-42803. doi:10.1074/jbc.M112.419424
- Kubitza C, Bittner F, Ginsel C, Havemeyer A, Clement B, Scheidig AJ. Crystal structure of human mARC1 reveals its exceptional position among eukaryotic molybdenum enzymes. *Proc Natl Acad Sci USA.* 2018;115(47):11958-11963. doi:10.1073/pnas.1808576115
- Moggridge S, Sorensen PH, Morin GB, Hughes CS. Extending the compatibility of the SP3 paramagnetic bead processing approach for proteomics. *J Proteome Res.* 2018;17(4):1730-1740.
- Feng D, Wang J, Yang W, et al. Regulation of Wnt/PCP signaling through p97/VCP-KBTBD7-mediated Vangl ubiquitination and endoplasmic reticulum-associated degradation. *Sci Adv.* 2021;7(20):eabg2099.
- Pandey S, Djibo R, Darracq A, et al. Selective CDK9 inhibition by natural compound toyocamycin in cancer cells. *Cancer.* 2022;14(14):3340.
- Gallagher CM, Garri C, Cain EL, et al. Ceapins are a new class of unfolded protein response inhibitors, selectively targeting the ATF6 α branch. *Elife.* 2016;5:e11878.

25. Axten JM, Medina JR, Feng Y, et al. Discovery of 7-methyl-5-(1-[[3-(trifluoromethyl) phenyl] acetyl]-2, 3-dihydro-1 H-indol-5-yl)-7 H-pyrrolo [2, 3-d] pyrimidin-4-amine (GSK2606414), a potent and selective first-in-class inhibitor of protein kinase R (PKR)-like endoplasmic reticulum kinase (PERK). *J Med Chem*. 2012;55(16):7193-7207.
26. He S, McPhaul C, Li JZ, et al. A sequence variation (I148M) in PNPLA3 associated with nonalcoholic fatty liver disease disrupts triglyceride hydrolysis. *J Biol Chem*. 2010;285(9):6706-6715.
27. Bozidis P, Williamson CD, Colberg-Poley AM. Isolation of endoplasmic reticulum, mitochondria, and mitochondria-associated membrane fractions from transfected cells and from human cytomegalovirus-infected primary fibroblasts. *Curr Protoc Cell Biol*. 2007;37(1):3.27.1-3.27.23.
28. Nicoletti A, Kaveri S, Caligiuri G, Bariéty J, Hansson GK. Immunoglobulin treatment reduces atherosclerosis in apo E knock-out mice. *J Clin Invest*. 1998;102(5):910-918.
29. Martinez-Forero I, Rouzaut A, Palazon A, Dubrot J, Melero I. Lysine 63 polyubiquitination in immunotherapy and in cancer-promoting inflammation. *Clin Cancer Res*. 2009;15(22):6751-6757.
30. Zhao L, Zhao J, Zhong K, Tong A, Jia D. Targeted protein degradation: mechanisms, strategies and application. *Signal Transduct Target Ther*. 2022;7(1):113.
31. Li H, Sun S. Protein aggregation in the ER: calm behind the storm. *Cell*. 2021;10(12):3337.
32. Struwe MA, Clement B, Scheidig A. The clinically relevant MTARC1 p. Ala165Thr variant impacts neither the fold nor active site architecture of the human mARC1 protein. *Hepatol Commun*. 2022;6(11):3277-3278.
33. Ott G, Plitzko B, Krischkowski C, et al. Reduction of sulfamethoxazole hydroxylamine (SMX-HA) by the mitochondrial amidoxime reducing component (mARC). *Chem Res Toxicol*. 2014;27(10):1687-1695.
34. Ott G, Reichmann D, Boerger C, et al. Functional characterization of protein variants encoded by nonsynonymous single nucleotide polymorphisms in MARC1 and MARC2 in healthy Caucasians. *Drug Metab Dispos*. 2014;42(4):718-725.

SUPPORTING INFORMATION

Additional supporting information can be found online in the Supporting Information section at the end of this article.

How to cite this article: Dutta T, Sasidharan K, Ciociola E, et al. Mitochondrial amidoxime-reducing component 1 p.Ala165Thr increases protein degradation mediated by the proteasome *Liver Int*. 2024;44:1219-1232. doi:[10.1111/liv.15857](https://doi.org/10.1111/liv.15857)